

# Development of a Bonner sphere spectrometer with emphasis on decreasing the contribution of scattering by using a new designed shadow cone

Rahim Khabaz · S. Hashem Miri

Received: 19 April 2011 / Published online: 19 May 2011  
© Akadémiai Kiadó, Budapest, Hungary 2011

**Abstract** In this study, the Bonner sphere spectrometer (BSS) used for measurement of neutron spectra based a  $\text{BF}_3$  long counter. The most important problem for this system was a high count of scattered neutrons. This spectrometer was established by designed a new shadow cone with a smaller length and improved attenuation coefficient. Because of shortening the length of the shadow cone, distance of source and center of the sphere was decreased. Furthermore, external part of the thermal detector was covered with a suitable layer to reduce the contribution count of scattering neutrons. Experimental results show that BSS system with  $\text{BF}_3$  long cylindrical counter, applying the proper developments, can be used in neutron fluence spectrometry.

**Keywords** Neutron spectrometry · Bonner sphere · Shadow cone method · Monte Carlo calculation · Scattered neutrons

## Introduction

Application of neutron fields in areas of physics, engineering, medicine, nuclear weapons, petroleum exploration, biology, chemistry, nuclear power and other industries has increased during recent years [18]. Because of the importance of neutron spectrometry in workplaces

within nuclear facilities, Knowledge of spectrometric information is very helpful for correct evaluation of the readings of neutron dosimeters. These results can be applied for determination of both ambient dose equivalent and, if angular information about the field is available, personal dose equivalent (and effective dose) using tabulated fluence to dose equivalent conversion coefficients [10, 16, 20].

In spite of the poor resolution of the Bonner sphere spectrometer (BSS) it has played a very important role in the field of neutron spectrometry, especially in radiation protection monitoring for neutrons. The BSS, which was first described by Bramblett et al., consists of a thermal neutron sensor located in the centre of a number of different diameter polyethylene spheres [2, 5]. This spectrometer has the advantage that using simple electronic circuits and neutron fluxes can be detected in the presence of gammas and the sensitivity of these detectors is moderately high for neutrons [8, 9, 14, 17]. The energy range of neutron detection for this spectrometer is from thermal to GeV neutrons.

In the present work, we have evaluated the suitability of long  $\text{BF}_3$  for BSS. Although, this system needed some improvements to reduce the scattered neutrons were counted. The set of Bonner spheres used in this study consists of seven polyethylene spheres, with outer diameters of 3.5", 4.2", 5", 6.5", 8", 10" and 12". The thermal neutron detector is a long proportional counter filled with  $\text{BF}_3$  gas partial pressure of 0.92 atm.

For the complete set of seven configurations of the spectrometric system, the energy response functions have been obtained by Monte Carlo simulation included a detailed description of the geometry, using the MCN P4C by neutrons with energies between thermal and 20 MeV [6].

R. Khabaz (✉)  
Physics Department, Faculty of Sciences, Golestan University,  
49138-15739 Gorgan, Iran  
e-mail: r.khabaz@gu.ac.ir; ra\_khabaz@yahoo.com

S. H. Miri  
Physics Department, School of Sciences, Ferdowsi University  
of Mashhad, 91775-1436 Mashhad, Iran

This set-up had a very significant difficult in neutron spectrometry, that it was great counting for scattered neutrons. The first action was reducing the distance between the neutron source and sphere, and it also involves reducing the length of the shadow cone. So, by using Monte Carlo calculation a new shadow cone was designed with a shorter length than what was reported in the international organization for standardization [11]. As well as, the tail end of sensor which was left out of the moderator, was covered with an appropriate layer can absorb scattered neutrons. Finally, the improved system for neutron spectrometry was studied experimentally.

### The response functions

The response functions to neutrons were obtained by calculations. The MCNP4C Monte Carlo code and ENDF/B-VI neutron cross section data library were employed to calculate the response functions. Calculations for each configuration were performed at 26 energy points from thermal to 20 MeV, while a simplified spherical geometry was used for polyethylene moderator (with density of  $0.96 \text{ g/cm}^3$ ); the detailed geometry of the  $\text{BF}_3$  counter was simulated in this case. The  $\text{BF}_3$  wall was made of copper with 0.89 mm thickness, and the effective length of this counter was 25.4 cm with the height of 28.2 cm, and also the pressure of gas filling of  $\text{BF}_3$ , according to the manufacture, was 0.92 atm at 293 K. In this detector enrichment of  $^{10}\text{B}$  was about 96%. The neutron source consisted of a disk source having the same diameter of the sphere under study, emitting a mono-energetic parallel neutron beam toward the sphere. The space between the neutron source and the BSS was assumed to be a vacuum.

The calculation of the response was accomplished being selected the tally F4 of MCNP4C, being considered the  $(n, \alpha)$  reaction, associated to a card multiplier that contains the volume of the detector, the area of the disk source and the atom density (atom/barn cm) of  $\text{BF}_3$ .

The calculated response functions are presented in Fig. 1. Error bars were omitted to prevent clutter. The uncertainty of most calculated values is below 1 or 2%, but it reached up to 4% or in a few cases.

The responses first increase, reach a maximum, and then decrease. The reduced response of spheres at low neutron energies is due to capture of thermalized neutrons in the hydrogen of polyethylene. Also, decrease of the response in high energies is due to escape of neutrons from the polyethylene sphere.

The response of the 3.5'' sphere is the one with its peak position at the lowest energy. The bigger sphere, the higher is the energy of the peak position on the energy scale. With increasing the diameter of sphere, the maximum of the

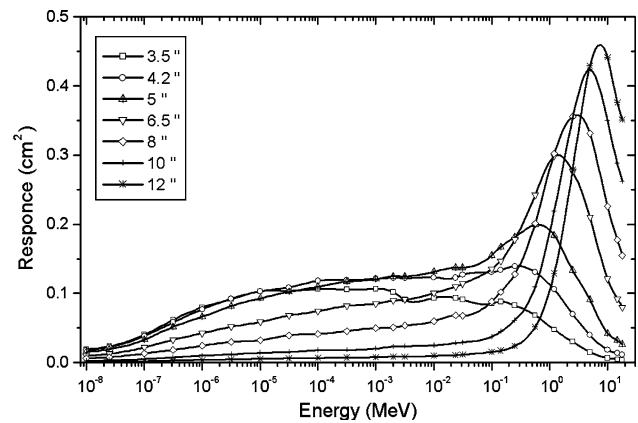


**Fig. 1** Energy response functions of the whole BSS with  $\text{BF}_3$  long cylindrical counter inside calculated with MCNP4C

response function grows and the energy of the peak position is only slightly increasing in logarithmic energy scale. Although the scale of the diagram is large, it may be concluded that the response values below  $10^{-7}$  MeV are very low (less than  $0.04 \text{ cm}^2$ ). Response functions of spheres with  $\text{BF}_3$  are very similar in the low-energy beginning, and their relative ratio for energies below  $10^{-7}$  MeV exhibits very little variation.

### Corrections for contribution of scattering

For point detector and an isotopic point source in an evacuated space, the product  $CD^2$  is a constant, where  $C$  is the dead-time corrected count rate of the detector, induced by the source at a separation distance  $D$ . This product is sometimes called the characteristic constant for the particular source-detector combination. A general functional relationship for the detector reading in free space,  $C(D)$ , at a separation distance between the neutron source and center of BSS,  $D$ , is given by

$$C(D) = \frac{KF_1(D)F_2(\theta)F_3(D)}{D^2} \quad (1)$$

The function  $F_1(D)$  is the geometry correction (represents the additional number of neutrons entering a spherical device compared with an irradiation by a plane-parallel beam) that in this work considered close to unit [3];  $F_2(\theta)$  is the anisotropy factor for emission of source,  $F_3(D)$  is the total air and room scattering correction factor, and  $K$  is the source-detector characteristic constant.

Air scattering generally the amount to only a few percent, and the source anisotropy may be very small. However, since the albedo of fast neutrons from concrete and other building materials is great [1]. The contribution of room-reflected neutrons to the response of the detector may be significant, particularly if the counter is sensitive to the

low energy neutrons resulting from the room scatter. These scattered neutrons have a different spectrum and a different variation with distance from the source. Therefore, they must not be considered a proper part of the calibration field but should rather be considered a type of background, and appropriate correction made [7].

Reasonable calibration procedures require that the instrument reading be corrected for all effects that may influence it, including neutron scattering by air, the walls, floor and ceiling of the calibration room. There are many techniques that have been used to evaluate scattering corrections necessary for proper calibration of neutron spectrometer instruments, one of which is shadow cone technique. This technique relies upon the experimental determination of the scattered components, due to both walls reflected and air-scattered neutrons, using a shadow cone designed to prevent any neutrons passing directly from the source to the detector.

Geometry-correction factor for the finite source or detector size in order to tend to unit, generally measurements are made at a distance of more than twice the shadow cone length [11]. One particular design of the shadow cone consists of two parts: a front end, with the length of 20 cm entirely made of iron; and a rear section, with the length of 30 cm made of polyethylene [12].

A Monte Carlo calculation was performed based on the BSS equipped with  $\text{BF}_3$  long counter, for evaluation of the amount of scattered neutrons in Nuclear Laboratory of the Ferdowsi University of Mashhad ( $11.5 \text{ m} \times 9.0 \text{ m} \times 4.0 \text{ m}$ ) with 40 cm concrete walls. The separation distance between the neutron source and center of each polyethylene sphere was 115 cm. For calculating the scattering contribution, the shadow cone (30 cm polyethylene and 20 cm iron) was placed between neutron source and sphere, while distance between the center of sphere and the back face of the cone was 50 cm. To determine the best height of the system from floor, with minimum contributions of scattering neutron, a  $^{241}\text{Am}$ -Be neutron source [13] was considered at the center of laboratory in several heights, at disposal of an 8" BSS. The result of calculation for this simulation is shown in Fig. 2, which total count is due to direct and scattered neutrons. The count was for  $10^6$  neutrons emitted from isotropic  $^{241}\text{Am}$ -Be source.

It can be observed that the height of 210 cm has a lowest counting. It is due to decline of counted for neutron scattered.

In these conditions, the ratio of the scattered neutrons to direct neutrons for small spheres (3.5", 4.2" and 5") was more than 2.05, while it is expected to be less than 0.4 [11]. To overcome the problem, first should be recognized the factors that will be caused increase the scattering count. For reducing the scattering count in this set-up, two processes were performed.

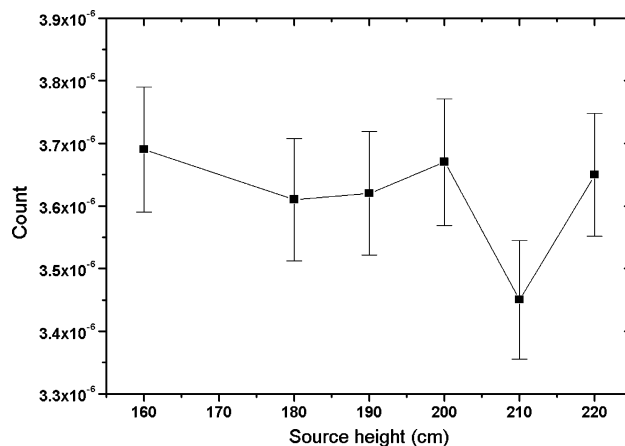


**Fig. 2** Total count (direct and scattered) for an 8" BSS in various heights of set-up from the floor

### Cover of the $\text{BF}_3$

Because of using the long counter, a lot of scattered neutrons arrived in the counter from a part of  $\text{BF}_3$  that was out of the sphere. To eliminate of this problem, external part of the  $\text{BF}_3$  can be covered with the proper layer, to absorb scattered neutrons. The scattered neutrons have lower energy than direct neutrons; therefore, the material of covering layer must be able to moderating and having a high absorb cross section in low energy. The hydrogen ( $^1\text{H}$ ) is the best element for moderate of neutrons, and also  $^{10}\text{B}$  has a great cross section for thermal neutrons; therefore, a layer of boric acid ( $\text{H}_3\text{BO}_3$ ) could be acceptable. The relative count of scattered neutrons from entering to external part of detector to total contribution of scattered neutrons for all spheres as a function of boric acid thickness is shown in Fig. 3.

As it can be seen in Fig. 3 the count of scattering neutrons is decreased with increase the thickness of boric acid.

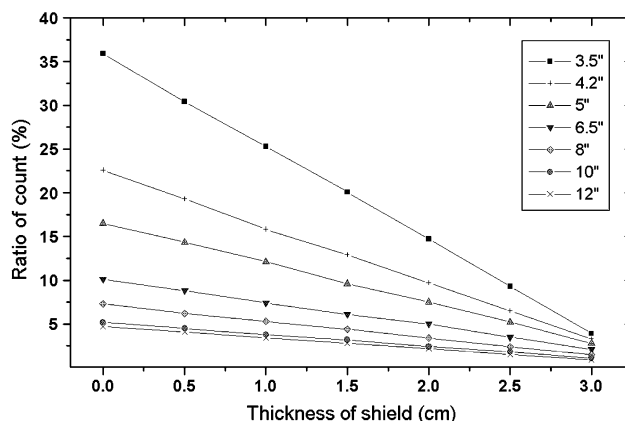


**Fig. 3** The percent relative count of scattered neutrons from entering to external part of  $\text{BF}_3$  to total contribution of scattered neutrons as a function of boric acid thickness

However, it should be noted that the outer radius of layer on  $\text{BF}_3$  must be smaller than the radius of smallest sphere (3.5"); then the 3 cm thickness of boric acid on the external part of detector is adequate to prevent scattered neutrons. It became clear that for this thickness, less than 4% of neutrons entered to external part of counter; thus it was not necessary to use other layers. For this condition ratio of the scattered neutrons to direct neutrons was declined from 2.05 to 1.23.

Decrease of the distance base on design a new shadow cone

The relative contribution of scattered neutrons to the reading compared to that of direct source neutrons may be reduced by performing the measurements at closer separation distances. There was a limitation for decrease of distance; the minimum distance separation between source and center of sphere should be twice the length of shadow cone. Therefore, it was necessary to design a new shadow cone with a shorter length than 50 cm. In first stage, materials of cone that were selected were: iron, water with 5% boric acid and pure boric acid.

The emitted neutrons from source arrive in iron, and they are moderated to lower energy due to inelastic scattering interaction. Then, neutrons enter to water (with 5% boric acid) and some of them are thermalized or absorbed by  $^1\text{H}$  and  $^{10}\text{B}$ . Finally, according to have a high capture cross section for  $^{10}\text{B}$ , thermalized neutrons are absorbed in boric acid.

This design must be performed to optimize the length, mass and attenuation coefficient of shadow cone. The total length of cone was considered 35 cm while the thickness of pure boric acid was 4 cm; then by Monte Carlo calculation thicknesses of iron and water were optimized with try and error. The simulation showed that a shadow cone by a front end, with the length of 17.0 cm constituted by iron, a middle section, with the length of 14.0 cm consisted of water with 5% boric acid, and a rear section, with the length of 4.0 cm, which was made of boric acid entirely has an agreement attenuation coefficient for source neutrons. Figure 4 illustrates the ratio of the attenuation coefficient for new cone (35 cm) to attenuation coefficient for old cone (50 cm). It can be seen, the new shadow cone has a smaller length but its attenuation coefficient is improved.

Using the new shadow cone, separation distance between the  $^{241}\text{Am-Be}$  source and center of sphere was considered 75.0 cm. In Fig. 5, ratios of scattered neutrons to direct neutrons were compared for all conditions: using old cone without boric acid on  $\text{BF}_3$ , using the old cone with boric acid on  $\text{BF}_3$  and applying the new cone with boric acid on  $\text{BF}_3$ .

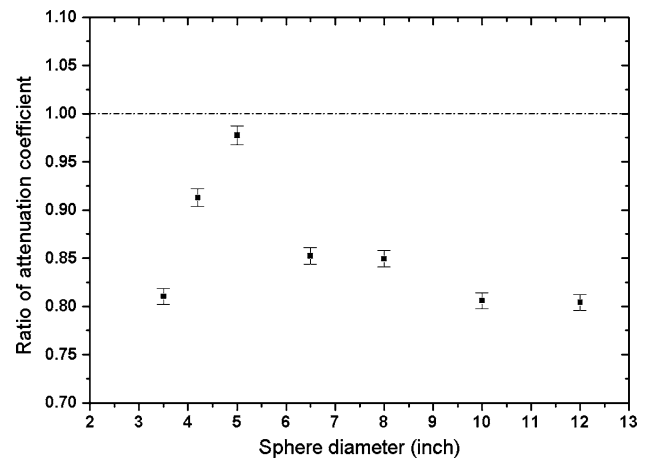


**Fig. 4** The ratio of attenuation coefficient for new cone (35 cm) to attenuation coefficient for old cone (50 cm)

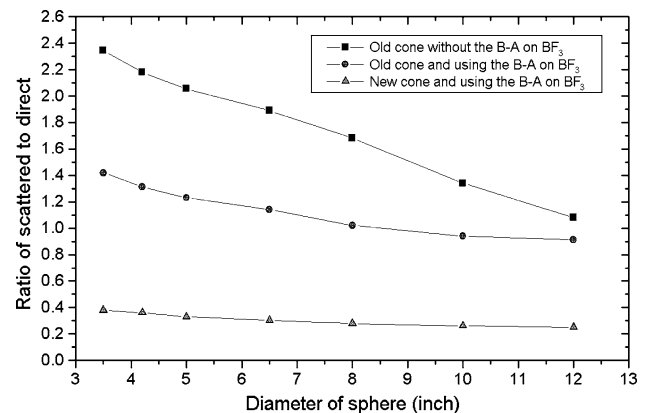


**Fig. 5** The ratios of scattered neutrons to direct neutrons in all spheres for different conditions

The MCNP calculation revealed that the ratio of the scattered neutrons to direct neutrons in this separation distance, for small spheres (3.5", 4.2" and 5") and large spheres (6.5", 8", 10" and 12") was less than 0.38 and 0.25 respectively.

### Validation experiment

The spectrometric performance of the new system has been evaluated by experiment using a known neutron-energy spectra. The BSS, used for  $^{241}\text{Am-Be}$  neutron source (50 mm  $\times$  30 mm) consists of seven polyethylene spheres, with a mean density 0.96 g/cm<sup>3</sup>. The thermal neutron counter, positioned at the centre of the spheres, is a long-cylindrical  $\text{BF}_3$  proportional counter of type 2210, manufactured by LND. BSS measurements were performed at the center of library (11.5 m  $\times$  9.0 m  $\times$  4.0 m), while the height of set-up from floor was 210 cm, and separation distance between source and center of spheres was 75 cm.

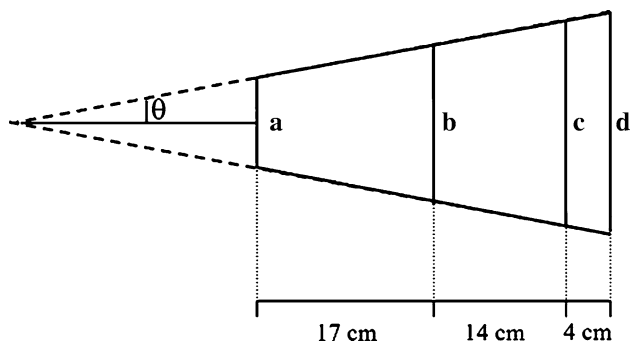


**Fig. 6** Applied new shadow cone: *a* front end, 17.0 cm length constituted by iron; a middle section, 14.0 cm length consisted of water with 5% boric acid; and a rear section, 4.0 cm length included of entirely boric acid (*a, b, c, d* and  $\theta$  were assigned in Table 1)

**Table 1** Geometry specifications of new shadow cones used in experimental set-up

	Spheres diameter	$\theta$ (°)	<i>a</i> (cm)	<i>b</i> (cm)	<i>c</i> (cm)	<i>d</i> (cm)
Cone (I)	3.5", 4.2", 5"	1.23	3.3	4.0	4.6	4.8
Cone (II)	6.5", 8"	2.70	3.6	5.2	6.5	6.9
Cone (III)	10", 12"	4.41	4.2	6.8	9.0	9.6

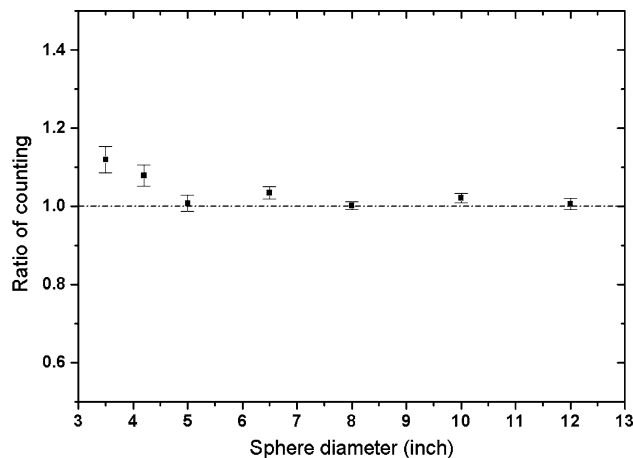
The separation of the neutron-induced events from pulses due to noise or gamma ray induced events was performed by introducing a discrimination threshold below the lower limit of the neutron induced pulse-height distribution in MCA, whilst rejection of noise pulses did not have too much effect on the neutron sensitivity.

In order to account for the scattered neutrons, the new designed shadow cone (with 35.0 cm length) was used between the source and sphere. The source-shadow cone distance was 5.0 cm. In this experiment, three types of new shadow cone with different obscured diameter were applied. Figure 6 and Table 1 give the geometric properties of these new shadow cones used in measurement of scattered neutrons.

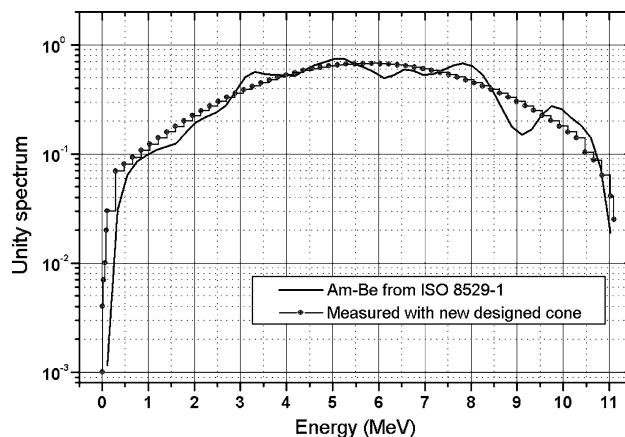
The cone (I) was used for 3.5", 4.2" and 5" spheres; the cone (II) was used for 6.5" and 8" spheres; the cone (III) was applied for 10" and 12" spheres.

Figure 7 indicates the ratio of direct neutrons measured in experiment by BSS to those calculated from the ISO standard neutron spectrum for <sup>241</sup>Am–Be.

It can be seen that measurement and the calculation are in good agreement if we consider the experimental errors. However, for some spheres this ratio is departure from one; this may be attributed to the overshadowing of these spheres during the measurement that this makes lower count for scattered neutrons.



**Fig. 7** The ratio of direct count from experiment to calculation



**Fig. 8** Comparison of unfolded neutron spectrum from experiment with standard <sup>241</sup>Am–Be spectrum

The results obtained by the BSS system were unfolded with a modified version of the code SANDII [15]. This code uses an iterative perturbation method to obtain a best-fit neutron flux spectrum for a given input set of measured detector counts. The procedure consists of a flux spectrum that serves as the initial approximation to a solution.

The direct counts of the <sup>241</sup>Am–Be source and energy response functions that have been calculated with MCNP, were used as input values in SANDII. Therefore, in this calculation the neutron spectrum is determined at position of the detector.

Figure 8 illustrates the experimental neutron spectrum of <sup>241</sup>Am–Be source that unfolded with the program SANDII, in comparison with ISO standard spectrum [13]. As it can be seen a satisfactory agreement has been obtained for the spectrum <sup>241</sup>Am–Be source using the new shadow cone, taking into account the low energy resolution of the BSS system [19].



**Table 2** Comparison of the fluence-average neutron energy

	$E_\phi$ (MeV)	$\frac{E_\phi - E_\phi(\text{ref.})}{E_\phi(\text{ref.})} \times 100$
Reference	4.16	0
With new cone	4.05	2.64
Bedogni report	4.24	1.92

The fluence-average neutron energy,  $E_\phi$ , was obtained as follows:

$$E_\phi = \int E\Phi(E)dE \quad (2)$$

where  $\Phi(E)$  is the neutron fluence. Table 2 presents the fluence-average neutron energy corresponding to this work for using new shadow cone, and compares them to the reference values and report of Bedogni et al. [4]. As it can be seen, the result of this set-up is in agreement with the reference.

## Result and discussion

A BSS system based on  $\text{BF}_3$  long cylindrical proportional counter has been developed. The energy response functions of the spectrometer have been accurately simulated from  $10^{-8}$  to 20 MeV neutrons. The main goal of this work was the evaluation of a BSS with emphasis on decreasing the contribution of scattering. To decrease the scattered neutrons, the rear part of the  $\text{BF}_3$  long counter that is out of sphere has been covered with 3.0 cm boric acid. In the next step, with design a smaller shadow cone, the separation distance between the neutron source and sphere was decreased.

An experimental validation containing seven spheres and applying the new shadow cone for calibration has been performed with  $^{241}\text{Am}$ -Be source in the laboratory. Although the BSS system has inherently poor energy resolution, the results shown herein indicate a satisfactory agreement; as the deviation of fluence-average neutron energy from the reference value is low. Therefore, the BSS system that has been equipped with  $\text{BF}_3$  long cylindrical counter with some improvements is acceptable for neutron fluence spectrometry.

## References

- Allen FJ, Futterer A, Wright W (1963) Dependence of neutron albedos upon hydrogen content of a shield. Ballistic Research Laboratories Report BRL-1224, Aberdeen
- Awschalom M, Sanna RS (1985) Applications of Bonner sphere detectors in neutron field dosimetry. *Radiat Prot Dosim* 10: 89–101
- Axton EJ (1972) The effective centre of a moderating sphere when used as an instrument for fast neutron flux measurement. *J Nucl Energy* 26:581–583
- Bedogni R, Domingo C, Esposito A, Fernández F (2007) FRUIT: an operational tool for multisphere neutron spectrometry in workplaces. *Nucl Instrum Methods A* 580:1301–1309
- Bramblett RL, Ewing RI, Bonner TW (1960) A new type of neutron spectrometer. *Nucl Instrum Methods* 9:1–12
- Briesmeister JF (2000) MCNP—a general monte carlo N-particle transport code. Version 4C. Los Alamos National Laboratory Report LA-13709-M, Los Alamos
- Eisenhauer CM, Hunt JB, Schwartz RB (1985) Calibration techniques for neutron personal dosimetry. *Radiat Prot Dosim* 10:43–57
- Green T, Biegalski S, O'Kelly S, Sayre G (2008) Neutron energy spectrum determination and flux measurement using MAXED, GRAVEL, and MCNP for RACE experiments. *J Radioanal Nucl Chem* 276:279–284
- Hakim M, Zahir I, Tassadit S, Malika A (2010) MCNP5 evaluation of a response matrix of a Bonner sphere spectrometer with a high efficiency  $^6\text{LiI}$  (Eu) detector from 0.01 eV to 20 MeV neutron. *J Radioanal Nucl Chem* 284:253–263
- ICRP (2007) The 2007 recommendations of the International Commission on Radiological Protection. Elsevier Health Sciences/Pergamon Press, Oxford
- ISO 10647 (1996) Procedure for calibrating and determining the response of neutron-measuring devices used for radiation protection purposes. International Organization for Standardization, Geneva
- ISO 8529-2 (2000) Reference neutron radiations—part 2: calibration fundamentals of radiation protection devices related to the basic quantities characterizing the radiation field. International Organization for Standardization, Geneva
- ISO 8529-1 (2001) Reference neutron radiations—part 1: characteristic and methods of productions. International Organization for Standardization, Geneva
- Jacobs GJH, van den Bosch RLP (1980) Calibration measurements with the multisphere method and neutron spectrum analyses using the SAND-II program. *Nucl Instrum Methods* 175:483–489
- Mc Elroy WN, Berg S, Crockett T, Hawkins RG (1967) A computer automated iterative method for neutron flux spectra determination by foil activation. Report AFWL-TR-67-41, Air Force Weapon Laboratory, Kirtland
- Miri-Hakimabad H, Rafat-Motavalli L, Karimi-Shahri K (2009) Assessment of neutron fluence to organ dose conversion coefficients in the ORNL analytical adult phantom. *J Radiol Prot* 29:51–60
- Thomas DJ, Bardell AG, Macaulay E (2002) Characterisation of a gold foil based Bonner sphere set and measurements of neutron spectra at a medical accelerator. *Nucl Instrum Methods A* 476:31–35
- Vega-Carrillo HR, Baltazar-Raigosa A (2011) Photoneutron spectra around an 18 MV LINAC. *J Radioanal Nucl Chem* 287:323–327
- Vega-Carrillo HR, Martinez-Blanco MR, Hernandez-Davila VM, Ortiz-Rodriguez JM (2009) Spectra and dose with ANN of  $^{252}\text{Cf}$ ,  $^{241}\text{Am}$ -Be,  $^{239}\text{Pu}$ -Be. *J Radioanal Nucl Chem* 281:615–618
- Vega-Carrillo HR, Ortiz-Hernandez A, Hernandez-Davila VM, Hernandez-Almaraz B, Teodoro RM (2010)  $\text{H}^*(10)$  and neutron spectra around LINACs. *J Radioanal Nucl Chem* 283:537–540